Journal of
Functional Biomaterials

MDPI

Article

Cross-Sectional Characterization of Stain Retention and Glaze Alteration in 3D-Printed and Milled Hybrid Dental Materials

Jamila Yassine [1,*], Florian Beuer [1], Sandi Debes [1,2] and Elisabeth Prause [1]

[1] Department of Prosthodontics, Geriatric Dentistry and Craniomandibular Disorders, Charité—Universitätsmedizin Berlin, Corporate Member of Freie Universität Berlin and Humboldt-Universität zu Berlin, Aßmannshauser Str. 4–6, 14197 Berlin, Germany; florian.beuer@charite.de (F.B.); sandi.debes@charite.de (S.D.); elisabeth.prause@charite.de (E.P.)
[2] Department of Prosthodontics, Medical Faculty and University Hospital Düsseldorf, Heinrich Heine University Düsseldorf, Moorenstraße 5, 40225 Düsseldorf, Germany
* Correspondence: jamila.yassine@charite.de

Abstract

Milled CAD/CAM and 3D-printed hybrid restorative materials are exposed to dietary staining agents, while polishing and glazing are used to optimize their surface and optical properties. This study characterized the cross-sectional location of visible staining and glaze alteration after prolonged staining exposure. Three milled and two 3D-printed hybrid materials were polished or glazed with OPTIGLAZE Color Clear HV and immersed in cola, coffee, curry, or red wine for 30 days at 37 °C. One specimen per material, surface treatment, and staining medium was sectioned (40 specimens in total). Stained glaze-layer thickness and glaze alteration were compared descriptively with previously reported color change and surface roughness. Polished specimens showed no distinct subsurface discolored zone. In glazed specimens, visible staining was located predominantly within the glaze layer and was measurable in 16 of 20 specimens (median 30.0 µm; range 14.4–63.8 µm). Curry exposure suggested near-surface yellowing in some materials, particularly beneath detached glaze. Structural defects were common, and partial detachment was observed in single specimens after curry or red wine exposure. Water-stored glazed controls showed no detachment and, where delineable, similar glaze thickness. In this descriptive analysis, cross-sectional evaluation revealed glaze alterations that were not consistently represented by surface measurements.

Keywords: CAD/CAM hybrid materials; 3D printing; glaze; staining; cross-sectional microscopy; color stability; surface roughness

Academic Editors: Claudia Barbosa, Tiago Reis, José Martín-Cruces and Benjamín José Martín

Received: 21 October 2026
Revised: 17 November 2026
Accepted: 19 November 2026
Published: 23 November 2026

Copyright: © 2026 by the authors. Licensee MDPI, Basel, Switzerland. This article is an open access article distributed under the terms and conditions of the Creative Commons Attribution (CC BY) license.

1. Introduction

Long-term esthetic stability is important for tooth-colored indirect restorations, which must retain their appearance despite repeated contact with saliva, dietary substances and oral hygiene procedures. In resin-containing CAD/CAM materials, the polymer phase can absorb water and interact with external staining compounds, contributing to clinically perceptible color changes [1–3]. Hybrid restorative materials combine a polymer matrix with an inorganic or ceramic phase, but their microstructure and filler architecture vary substantially [4]. These materials are produced not only by milling but increasingly by additive manufacturing, and printable hybrid resin-ceramic systems are

now available for definitive indirect restorations [5]. Numerous in vitro studies have evaluated staining of resin-based restorative materials after exposure to coffee, red wine, cola and other dietary media. Susceptibility to discoloration varies with material composition [6–8], type and duration of exposure [9–11], and finishing protocol [10,12–15]. Most studies quantify color change spectrophotometrically, commonly using CIEDE2000. Although such measurements capture the overall optical change at the restoration surface, they cannot distinguish whether staining is limited to the outer surface, retained within a coating, or extends into the restorative material. Light-curing glazes are often used to seal resin-based and 3D-printed restorations and may reduce water sorption and pigment uptake [16,17]. Some studies have reported lower roughness and improved color stability after glazing of 3D-printed permanent resins, but the effect depends on the material and surface-treatment protocol [18]. Recent reviews and experimental studies likewise show that post-processing, post-curing, surface finishing, printing orientation, restoration thickness, and chromogenic exposure can influence the optical and surface behavior of printed restorations [19–22]. At the same time, limited adhesion, non-uniform coating distribution and progressive degradation of surface coatings have been described [16,17,23]. In our preceding study using the same specimen set, all five glazed groups showed greater color change than the corresponding polished groups, while scanning electron microscopy revealed cracking and delamination of the glaze; surface roughness (arithmetic mean roughness, Ra) did not consistently parallel the observed discoloration [24]. Clinical findings from our group provide additional context. Glazed 3D-printed non-invasive restorations made from the ceramic-filled 3D-printed resin investigated here as 3D1 showed progressive loss of color stability over 24 months, and glaze detachment was proposed as a possible explanation although the coating itself was not examined [2]. Considerable occlusal wear was also documented in the same clinical setting [25]. These clinical findings motivated the present in vitro analysis using the same 3D-printed material and glazing system. This prompted the question of whether staining in glazed specimens is located primarily within the glaze and whether the condition of that layer is related to the observed surface color change. Cross-sectional microscopy enables direct visualization from the exposed surface toward the material interior. Previous work has used cross-sections to measure OPTIGLAZE thickness on 3D-printed resins and specifically highlighted the need to relate coating thickness to color stability [23]. In our preceding study, selected glazed VITA Enamic specimens were examined qualitatively in cross-section to illustrate staining and glaze degradation [24], but no systematic analysis across all five materials was performed. The primary objective of the present study was therefore to characterize the location of visible staining, the thickness of the visibly stained glaze layer and the condition of the glaze after 30 days of immersion in different staining media. A secondary objective was to compare these cross-sectional findings with the previously reported ΔE_{00} and Ra values for the same experimental groups [24].

2. Materials and Methods

2.1. Study Design and Materials

Five hybrid restorative materials were included: three milled CAD/CAM materials, VITA Enamic (VE; polymer-infiltrated ceramic network; VITA Zahnfabrik, Bad Säckingen, Germany), Grandio blocs (VG; resin nanohybrid composite; VOCO GmbH, Cuxhaven, Germany) and Cerasmart (CS; resin nanoceramic; GC Europe, Leuven, Belgium), together with two additively manufactured hybrid materials (3D1, 3D2). 3D1 and the glaze correspond to the material and glazing system used in previous clinical studies from our group [2,25]. Material compositions are summarized in Table 1. As in the preceding study of the same specimen set [24], the trade names of the two 3D-printed materials are not disclosed; their classification, filler type, and filler content according to the manufacturer are given

https://doi.org/10.3390/jfb17120595

in Table 1. The specimens were obtained from the preceding investigation of color stability and surface roughness [24]; therefore, fabrication, surface treatment, and immersion procedures are summarized only briefly below.

Table 1. Restorative materials investigated. PICN, polymer-infiltrated ceramic network; DLP, digital light processing.

Code	Material	Classification	Composition (Manufacturer Data)
VE	VITA Enamic	Milled PICN	Feldspathic ceramic network (86 wt%) infiltrated with UDMA/TEGDMA polymer (14 wt%)
VG	Grandio blocs	Milled resin nanohybrid composite	86 wt% inorganic fillers (20–60 nm) in UDMA/DMA matrix
CS	Cerasmart	Milled resin nanoceramic	71 wt% fillers (SiO_2, Ba glass); 29 wt% Bis-MEPP, UDMA, DMA
3D1	3D-printed material 1	3D-printed hybrid (DLP)	30–50 wt% silanized dental glass (~0.7 µm) in methacrylate matrix
3D2	3D-printed material 2	3D-printed hybrid (DLP)	Methacrylate-based matrix with ~50 wt% inorganic fillers

2.2. Specimen Fabrication, Surface Treatment and Immersion

Disc-shaped specimens were fabricated either by milling (K5, vhf camfacture, Ammerbuch, Germany) or by DLP printing (Varseo XS, BEGO). Printed specimens were produced at a 90° orientation with a 50 µm layer thickness, cleaned ultrasonically in 96% ethanol for 3 min, rinsed with fresh ethanol and dried with oil-free compressed air, air-abraded with 50 µm particles at 1.5 bar, and post-cured in an Otoflash unit (BEGO; 1500 flashes per side). All specimen surfaces were sequentially ground with 320- to 1200-grit SiC paper under water cooling, cleaned in an ultrasonic bath with distilled water for 5 min and dried with oil-free compressed air. Within each material, specimens were finished either by polishing (Universal Polishing Paste, Ivoclar, Schaan, Liechtenstein) or by application of OPTIGLAZE Color Clear HV (GC, Tokyo, Japan) with a brush followed by light curing according to the manufacturer's instructions. Specimens were then immersed for 30 days at 37 °C in cola (River Cola Classic, ALDI Nord, Germany), instant coffee (Jacobs Krönung, Jacobs Douwe Egberts, Bremen, Germany), curry powder (Le Gusto, ALDI Süd, Germany), red wine (Doppio Tratto Primitivo IGT, Apulia, Italy), or distilled water while agitated on an orbital shaker (ES-20, bioSan, Riga, Latvia; 70 rpm). Each specimen was immersed individually in a tube containing 20 mL of solution. Coffee was prepared according to the manufacturer's instructions by dissolving 2.5 g of instant coffee in 250 mL of freshly boiled water (10 g/L). The curry suspension was prepared by dispersing one level teaspoon (approximately 2 g) of curry powder in 400 mL of water, corresponding to an estimated concentration of approximately 5 g/L. Cola and red wine were used undiluted. Solutions were replaced every 2 days [24]. Specimens were immersed directly after surface finishing, without pre-immersion conditioning in water or artificial saliva. After immersion, specimens were air-dried without rinsing or brushing to preserve the post-immersion surface. The 30-day immersion period was chosen as an accelerated worst-case staining challenge. Based on the commonly used extrapolation that 24 h of immersion corresponds to approximately one month of beverage consumption [26], it approximates about 2.5 years of dietary exposure and thus covers the 24-month observation period of the clinical studies on the same 3D-printed material [2,25].

2.3. Cross-Sectional Specimen Preparation

Following immersion, one representative specimen from each material × surface treatment × staining medium combination was sectioned centrally and perpendicular to the treated surface (40 specimens in total, one per group). In addition, one glazed specimen per material that had been stored in distilled water for 30 days under the same conditions was sectioned in the same way and served as an unstained, water-stored control (five specimens in total). Sectioning was performed under water cooling, and the sections were air-dried before microscopy. Because sectioning is destructive and the specimens originated from a previously completed immersion study [24], one representative specimen per group was sectioned. The use of one cross-sectional specimen per group is consistent with a previous evaluation of OPTIGLAZE layers on 3D-printed resins [23]. The cross-sectional analysis was therefore designed as a descriptive investigation, and no inferential comparisons among materials or staining media were performed.

2.4. Cross-Sectional Microscopy

Cross-sections were examined with a laser scanning confocal microscope (VK-X3000, Keyence, Osaka, Japan) using a 50× objective (NA 0.8) at optical zoom factors of 1.0 or 1.5, depending on the required field of view. Images were acquired with the VK-X3000 Viewer software, and thickness measurements were performed with the VK-X3000 MultiFileAnalyzer (VK-X3000 Software, version 3.3.1.85; Keyence). All images were acquired in color mode with identical settings for all specimens (light intensity, fixed white balance, high dynamic range disabled, default edge-enhancement filter), whereas exposure was adjusted automatically by the microscope software. Light-optical color imaging was chosen because the staining was defined by its visible color, which cannot be depicted by scanning electron microscopy (SEM), and because the calibrated measurement function allowed thickness measurements directly on the color images. The polished and glazed surfaces of the same specimen set were previously examined by SEM (Phenom XL G2 Desktop, Thermo Fisher Scientific, Waltham, MA, USA; low-vacuum mode, backscattered electron detector) [24]; representative SEM images of all groups are provided in the Supplementary Materials (Figure S10).

2.5. Thickness of the Stained Glaze Layer

When a distinct stained surface layer was present, its thickness was measured perpendicular to the specimen surface from the outer surface to the lower boundary of the discolored layer using the calibrated measurement function of the microscope software on the original images. Between one and four measurements were obtained per specimen (29 measurements in total), and the specimen-level mean was used for analysis. In the control specimens, the thickness of the unstained glaze layer was measured in the same way. Measurements with an indistinct lower boundary were flagged. Because no separate discolored zone could be identified visually beneath the glaze or in polished specimens, this variable is referred to as stained glaze layer thickness and should not be interpreted as penetration depth into the restorative substrate.

2.6. Cross-Sectional Glaze Alteration Score

Each glazed cross-section was assigned an ordinal glaze alteration score: 1, superficial alteration without a distinct layer; 2, continuous stained glaze layer with an intact contour; 3, stained glaze layer with structural defects such as cracking, segmentation, pores, or markedly variable thickness; and 4, partial or extensive glaze detachment, defined by a gap or lifting at the glaze–substrate interface. Scoring was initially performed by one examiner (J.Y.). To assess reproducibility, a second examiner (E.P.), blinded to material and staining medium, independently scored one representative image of each

glazed specimen. Inter-examiner agreement was expressed as exact agreement and Cohen's kappa (unweighted and linearly and quadratically weighted). The original scores were retained, and inter-examiner agreement is reported as a measure of reliability. The score was used as a descriptive morphological assessment. Polished specimens were described qualitatively because no glaze had been applied to these specimens and the glaze-related categories were therefore not applicable.

2.7. Image-Based Color Profiles

To explore substrate color changes that were not visually obvious, depth-dependent color profiles were derived from the cross-sectional images shown in Figures 1 and 2. Images were converted to CIELAB (D65), the specimen surface was detected on a column-wise basis, and mean L*, a*, and b* values were calculated in 2 μm increments to a depth of 120 μm. For each specimen, a near-surface substrate zone (2–20 μm beneath the stained glaze layer or, for polished specimens, beneath the surface) was compared with a deeper reference zone (80–110 μm). When no glaze thickness could be measured, the median stained-layer thickness of 30 μm was used as the assumed boundary. Differences were expressed as Δb* (yellowness) and Δa* (redness). Because the microscope images were not colorimetrically calibrated and exposure was adjusted automatically for each image, absolute color values were not compared between images; only relative within-image patterns were interpreted, and the analysis was considered exploratory. The profiles were not intended to quantify chromogen penetration but to identify relative near-surface color gradients for further investigation.

2.8. Color Change and Surface Roughness Data

Previously reported color change (ΔE_{00}, CIEDE2000) and arithmetic mean surface roughness (Ra) data from the same experimental groups [24] were used solely for descriptive comparison with the present cross-sectional findings. In the preceding study, color was measured with a VITA Easyshade V spectrophotometer, and ΔE_{00} was calculated relative to the mean of the distilled-water specimens within each material × surface-treatment group. Ra was measured using a laser scanning confocal microscope (VK-X3000, Keyence). Values are reported as group mean ± standard deviation.

2.9. Data Analysis

Cross-sectional data were summarized descriptively. Stained glaze layer thickness was reported as median and range, and glaze alteration scores were summarized as frequencies. Because only one specimen represented each material × surface treatment × staining medium combination, no inferential comparisons among materials or staining media were performed. Associations between stained glaze layer thickness and the previously reported group-mean ΔE_{00} and Ra values [24] were explored using Spearman rank correlation; p values were interpreted descriptively. Statistical analyses were performed in R (version 4.3.3; R Foundation for Statistical Computing, Vienna, Austria). Image-based color profiles were generated in Python (version 3.13) using scikit-image (version 0.26). Cohen's kappa was calculated in Python using scikit-learn (version 1.9). The Python script used for the image-based color profile analysis was reviewed and verified by the authors.

3. Results

3.1. Cross-Sectional Morphology

Figure 1 summarizes the cross-sections of all glazed specimens, and Figure 2 those of all polished specimens; side-by-side comparisons of polished and glazed specimens for each material are provided in the Supplementary Materials (Figures S2–S6). None of the

polished specimens showed a clearly demarcated discolored zone beneath the treated surface. In the glazed specimens, a continuous superficial layer was visible and showed medium-specific discoloration: brown after coffee, violet after red wine, yellow-green after curry, and gray after cola. On routine cross-sectional inspection, the substrate beneath this layer showed no distinct visible discoloration. Glaze alterations included cracking, segmentation, irregular thickness, and, in some specimens, a gap or lifting at the glaze–substrate interface (Figure 1).

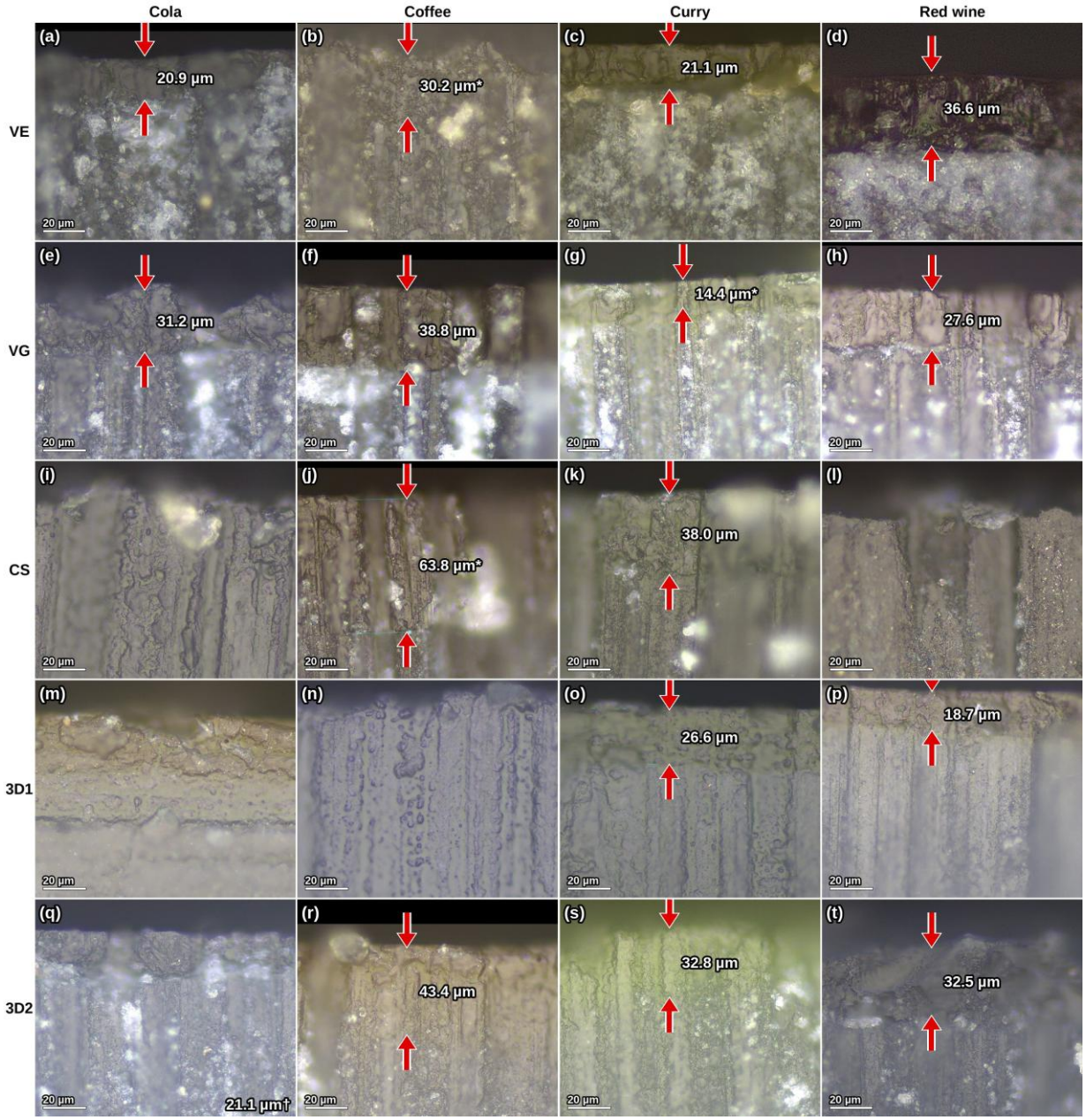

Figure 1. Cross-sectional micrographs (VK-X3000, 50× objective) of glazed specimens after 30 days of immersion. Columns show the staining media and rows the materials: (**a**–**d**) VE, (**e**–**h**) VG, (**i**–**l**) CS, (**m**–**p**) 3D1 and (**q**–**t**) 3D2. Red arrows mark the outer surface and the lower boundary of the stained glaze layer; values give the thickness measured at the marked position. *, boundary not clearly delineable; †, thickness measured at another location of the same section. No value is shown where no distinct layer boundary could be measured. Partial glaze detachment (score 4) is present in (**c**,**g**,**t**). Scale bars: 20 µm.

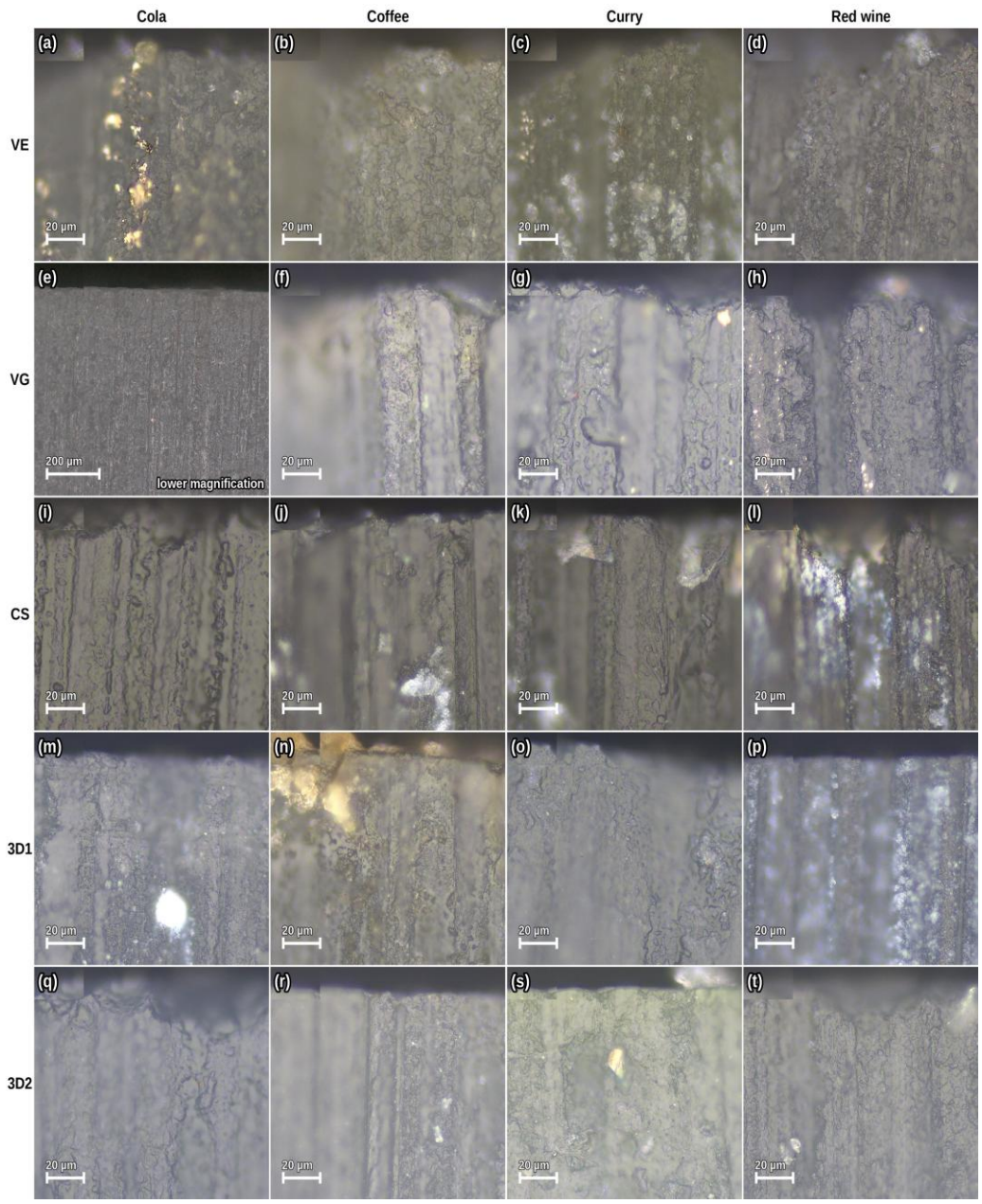

Figure 2. Cross-sectional micrographs (VK-X3000, 50× objective) of the polished specimens after 30 days of immersion. Columns show the staining media and rows the materials: (**a**–**d**) VE, (**e**–**h**) VG, (**i**–**l**) CS, (**m**–**p**) 3D1, and (**q**–**t**) 3D2. No distinct discolored zone is visible beneath the polished surface. Panel (**e**) was recorded at lower magnification because no 50× image was available for this specimen. Scale bars: 20 µm, except (**e**): 200 µm.

3.2. Stained Glaze Layer and Glaze Alteration

A stained glaze layer could be measured in 16 of the 20 glazed specimens (Table 2). Across these specimens, the median thickness was 30.0 µm (range 14.4–63.8 µm). Median thicknesses by staining medium were 21.5 µm for cola, 37.6 µm for coffee, 28.5 µm for curry and 29.6 µm for red wine. Considerable variation was also present within individual sections; for example, values ranged from 23.3 to 47.9 µm in 3D2 after coffee and from 12.5 to 24.5 µm in 3D1 after red wine.

In the water-stored glazed controls, the glaze appeared as a distinct, unstained surface layer in VG, 3D1 and 3D2 (Figure S1). Its mean thickness was 24.6 µm (range 19.4–31.7 µm) in VG, 29.2 µm (range 25.2–33.3 µm) in 3D1 and 25.1 µm (range 18.0–30.4 µm) in 3D2 and was thus within the range of the stained glaze layer measured after immersion.

In VE and CS, the boundary between glaze and substrate could not be reliably delineated in the control specimens. Irregular glaze contours and local variations in thickness were already present in the controls, whereas no gap or lifting at the glaze–substrate interface was observed in any control specimen.

Among the 20 glazed specimens, one was classified as score 1, six as score 2, ten as score 3, and three as score 4 (Table 2). Partial glaze detachment (score 4) occurred only after curry exposure in VE and VG and after red wine exposure in 3D2. The thinnest residual stained layer (14.4 µm) was measured in VG after curry, which also showed detachment. In the independent assessment by the second examiner, exact agreement was obtained in 8 of 20 specimens, and all disagreements differed by one category (unweighted $\kappa = 0.06$; linear weighted $\kappa = 0.25$; quadratic weighted $\kappa = 0.49$). The original scores were retained.

Table 2. Cross-sectional findings in glazed specimens and previously reported color change and surface roughness of the same groups. Stained glaze layer: mean of 1–4 measurements in the single sectioned specimen; –, not measured (no distinct layer boundary measured); *, boundary not clearly delineable. Glaze alteration score (original scores of the first examiner; for inter-examiner agreement, see Section 3.2): 1, superficial alteration; 2, continuous stained glaze layer; 3, stained layer with structural defects; 4, partial or extensive detachment. ΔE_{00} and Ra: mean ± SD of n = 5 specimens per group (n = 4 for ΔE_{00} of VG after curry), previously reported [24].

Material	Staining Medium	Stained Glaze Layer (µm)	Glaze Alteration Score	ΔE_{00} [24]	Ra (µm) [24]
VE	Cola	20.6	2	8.5 ± 1.9	0.50 ± 0.24
	Coffee	30.2 *	3	16.5 ± 1.5	0.51 ± 0.20
	Curry	21.1	4	20.7 ± 0.8	1.48 ± 0.72
	Red wine	36.6	3	25.2 ± 1.2	0.37 ± 0.09
VG	Cola	29.9	3	10.0 ± 0.8	0.14 ± 0.05
	Coffee	38.7	3	20.2 ± 0.7	0.39 ± 0.10
	Curry	14.4 *	4	19.6 ± 2.1	0.37 ± 0.20
	Red wine	26.8	2	23.4 ± 1.1	0.19 ± 0.04
CS	Cola	–	1	9.0 ± 1.8	0.21 ± 0.08
	Coffee	63.8 *	2	19.0 ± 0.9	0.30 ± 0.12
	Curry	40.8	3	20.0 ± 1.0	0.16 ± 0.11
	Red wine	–	2	19.8 ± 1.1	0.51 ± 0.18
3D1	Cola	–	3	10.5 ± 3.0	0.30 ± 0.41
	Coffee	–	2	15.3 ± 1.9	0.40 ± 0.26
	Curry	28.5	2	13.7 ± 2.1	0.12 ± 0.10
	Red wine	18.6	3	18.2 ± 0.7	0.44 ± 0.50
3D2	Cola	21.5	3	8.0 ± 1.6	1.25 ± 0.76
	Coffee	36.5	3	15.5 ± 1.0	0.36 ± 0.03
	Curry	34.9	3	18.6 ± 5.6	2.00 ± 0.70
	Red wine	32.5	4	20.0 ± 1.5	0.23 ± 0.11

3.3. Exploratory Color Profiles of the Near-Surface Substrate

The image-based profiles showed the largest near-surface b* gradients after curry exposure (Figure 3, Table S1). In glazed VE and VG, both of which showed partial glaze detachment, b* decreased progressively over approximately 30–60 µm from the glaze–substrate interface into the substrate ($\Delta b^* = +6.4$ and +8.1, respectively). Similar gradients were observed in glazed 3D2 ($\Delta b^* = +5.9$) and in polished VE and 3D2 ($\Delta b^* = +4.8$ and +7.7). In contrast, polished VG, CS and 3D1 and glazed CS and 3D1 showed little or no gradient ($\Delta b^* = -0.2$ to +2.0). In glazed 3D1, b* decreased sharply at the lower boundary of the glaze. After coffee exposure, b* gradients of similar magnitude were found in single specimens

(glazed 3D2 and polished VG and 3D1; Δb* = +4.4 to +6.2), whereas the remaining coffee specimens showed little or no gradient (Δb* = −0.1 to +3.1; Figure S8). No comparable redness gradient was observed after red wine exposure, including beneath the detached glaze of 3D2 (Δa* = −0.6 to +0.6; Figure S9). Cola produced smaller differences (Δb* = −1.5 to +2.9; Figure S7).

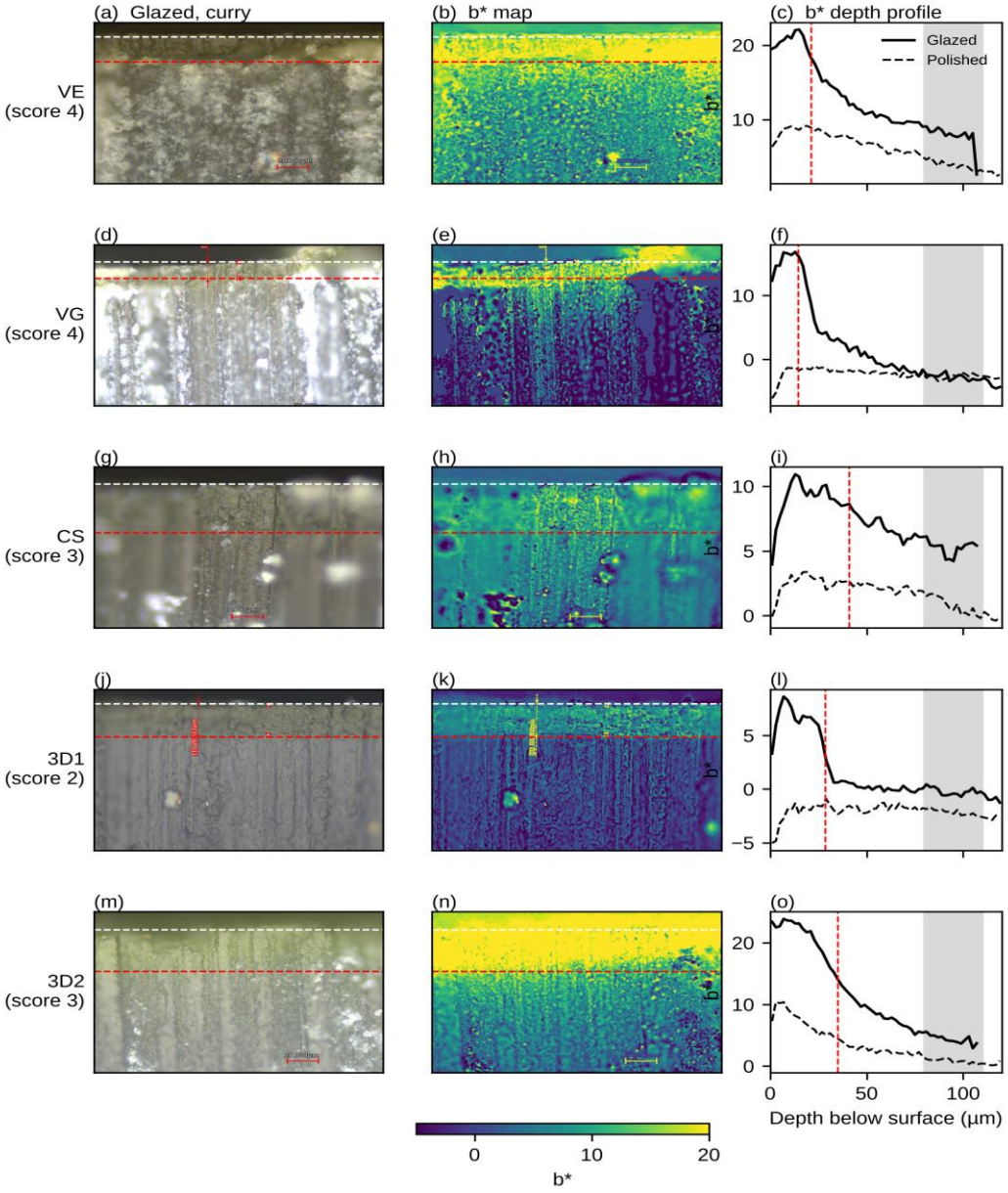

Figure 3. Exploratory color profiles after curry immersion: (a,d,g,j,m) glazed cross-sections of VE, VG, CS, 3D1 and 3D2, respectively; (b,e,h,k,n) b* maps (yellowness) from the same images; (c,f,i,l,o) b* depth profiles for the glazed (solid line) and polished (dashed line) specimens. The white dashed line marks the specimen surface, the red dashed line the measured lower boundary of the stained glaze layer, and the gray area the deep reference zone (80–110 µm). Glaze alteration scores are shown in brackets. Profiles were derived from uncalibrated microscope images and were interpreted only as relative within-image differences. Corresponding profiles for cola, coffee and red wine are shown in Figures S7–S9.

3.4. Relation to Previously Reported Color Change and Surface Roughness

Table 2 presents the cross-sectional findings together with the previously reported ΔE_{00} and Ra values for the same glazed groups [24]. The cola groups combined the

thinnest stained layers (median 21.5 µm) with the lowest ΔE_{00} values (8.0–10.5). For the remaining media, ΔE_{00} ranged from 13.7 to 25.2 without a consistent pattern in relation to stained-layer thickness. Groups with glaze detachment had ΔE_{00} values of 19.6–20.7, whereas the highest values occurred in VE and VG after red wine exposure (25.2 and 23.4, respectively) without detachment. Ra was highest in 3D2 after curry (2.00 µm), VE after curry (1.48 µm) and 3D2 after cola (1.25 µm), but remained at or below 0.37 µm in two of the three groups showing detachment. Exploratory Spearman correlations were $\varrho = 0.30$ ($p = 0.254$) for stained-layer thickness versus ΔE_{00} and $\varrho = -0.29$ ($p = 0.269$) for stained-layer thickness versus Ra (n = 16), indicating no clear association in this dataset.

4. Discussion

Cross-sectional evaluation showed that visible staining in glazed specimens was concentrated predominantly within the glaze layer, while polished specimens showed no distinct discolored subsurface zone. After curry exposure, exploratory image-based profiles suggested additional yellowing of the near-surface substrate in some materials, particularly beneath areas of detached glaze. Structural glaze defects were common, and detachment was observed in single specimens after curry and red wine exposure. Neither stained-layer thickness nor glaze detachment showed a consistent relationship with the previously reported ΔE_{00} or Ra values.

4.1. Location of Staining in Glazed Specimens

In the preceding study, all five glazed groups showed greater color change than their polished counterparts, and SEM demonstrated cracking and delamination of the glaze [24]. The present cross-sections help to interpret those findings by showing that the glaze itself can retain visible stain over a measurable thickness while the underlying substrate remains visually indistinct on routine inspection. The exploratory color profiles nevertheless suggested that curry-related yellowing may also be present in the near-surface substrate in selected materials. In VG, the b* gradient was present beneath detached glaze but not in the polished specimen, a pattern consistent with greater near-surface yellowing at the site of local glaze loss. However, these gradients were derived from uncalibrated images and may also partly reflect light scattering from the stained glaze into the translucent substrate as well as material-specific differences in translucency and microstructure; they should therefore not be regarded as evidence of chromogen penetration. In VE and 3D2, comparable gradients were also present in polished specimens, indicating that susceptibility to curry-related yellowing may partly depend on the restorative material itself rather than on the glaze alone. By contrast, the sharp decrease in b* at the glaze boundary in 3D1 suggests that the visible staining pattern remained largely associated with the glaze in this material. After coffee exposure, comparable b* gradients occurred only in single specimens without a consistent pattern across materials or surface treatments, so that no material- or treatment-specific tendency can be derived from these profiles. Because the glaze was visibly stained over a layer measuring several tens of micrometers, its optical contribution to the color recorded at the external surface may be substantial. This differs from studies in which glazing improved color stability. Nam et al. reported lower color change and Ra after glazing of 3D-printed permanent resins [18], whereas Lask et al. showed that the effects of glazing, coating, and polishing on discoloration and surface properties depend strongly on the restorative material and treatment protocol [16]. Narin and Ezmek also reported lower ΔE_{00} values for OPTIGLAZE-coated than for mechanically polished 3D-printed resins [23]. Their specimens were cleaned ultrasonically for 15 min before color measurement, whereas the specimens in the preceding study were measured without rinsing to preserve the post-immersion surface [24]. Differences in glaze application and curing, substrate composition, aging conditions and cleaning before color

measurement may therefore contribute to the different outcomes. These observations support treating the glaze as a distinct surface layer whose color behavior may differ from that of the underlying restorative material.

4.2. Glaze Alteration

In the single specimens examined, glaze detachment was observed only after curry and red wine exposure. Red wine combines low pH with ethanol, both of which may soften methacrylate networks and promote degradation of resin-based coatings [17,23]. Curry contains the lipophilic pigment curcumin, as well as a fat component that may interact with the polymer phase of the glaze, although this possibility requires direct experimental confirmation. Because only one specimen was sectioned for each group, these medium-specific observations should be interpreted descriptively. In addition, inter-examiner agreement for the glaze alteration score was only fair, so the distinction between adjacent categories, particularly between scores 2 and 3, should be regarded as approximate. Stained-layer thickness also varied markedly within individual sections; in 3D2 after coffee, for example, values ranged from 23 to 48 μm. Such variability may reflect non-uniform glaze application, local loss of the coating, or both. Narin and Ezmek reported OPTIGLAZE thicknesses of approximately 25–85 μm on 3D-printed permanent resins depending on whether glazing was performed before or after post-curing [23]. The stained glaze layers measured in the two 3D-printed materials in the present study (approximately 13–48 μm) were generally at the lower end of that range. In the water-stored controls, the thickness of the unstained glaze was within the range of the stained glaze layer after immersion. This indicates that the visible stain extended through most or all of the glaze thickness rather than being confined to its outer portion, and that pronounced thinning of the glaze during immersion was not evident in most groups. Irregular contours and local thickness variations were already present in the controls; part of the structural defects classified as score 3 may therefore reflect the initial glaze application rather than immersion-induced damage. In contrast, no detachment was observed in any control specimen, whereas detachment occurred after curry and red wine exposure, supporting an association between glaze detachment and these staining media.

4.3. Relation to Color Change and Surface Roughness

Stained glaze layer thickness did not show a consistent relationship with ΔE_{00}. Although the cola groups had both the lowest ΔE_{00} values and the thinnest stained layers, similar color changes were observed across the other media despite pronounced differences in layer thickness. The magnitude of surface color change therefore appears to depend on more than stained-layer thickness alone and may also reflect the staining agent, structural defects or partial loss of the glaze, and the optical properties of the underlying material. Because each thickness value came from a single sectioned specimen and was compared with a group mean, the exploratory correlations should be interpreted cautiously. Surface roughness likewise did not represent the cross-sectional state of the glaze: Ra remained low in two of the three groups with detachment. This agrees with the preceding study, in which Ra did not consistently parallel discoloration [24], and with reports that storage in coffee or acidic media did not significantly alter the roughness of CAD/CAM materials [27]. Recent data from glaze-coated 3D-printed resins similarly showed that roughness depended on material type rather than storage medium, while color change varied among material–medium combinations [22]. Cross-sectional evaluation may therefore provide information on glaze integrity that is not captured by roughness or surface color measurements alone.

4.4. 3D-Printed Versus Milled Materials

Across the present dataset, the two 3D-printed materials showed a broadly similar cross-sectional pattern to the milled materials. Visible staining was concentrated mainly within the glaze, while exploratory color profiles suggested curry-related near-surface yellowing in one printed material (3D2) and two milled materials (VE, VG). Glaze detachment was observed in single specimens of one printed material (3D2 after red wine) and of two milled materials (VE and VG after curry). Previous studies have shown that printing orientation and post-curing can affect color stability, gloss retention and surface properties of definitive filled 3D-printed resins [20,21], underscoring the process dependence of their optical behavior. Within the limits of the present sample, however, the cross-sectional findings did not indicate a specific disadvantage of the printed materials relative to the milled materials, consistent with the comparable color stability reported in the preceding study [24].

4.5. Clinical Relevance

The present findings can also be considered in the context of clinical studies from our group that used the same 3D-printed material as 3D1 and the same light-curing glaze [2,25]. In those restorations, the proportion rated alpha or bravo ($\Delta E \leq 3.7$) decreased from 55% after 6 months to 34% after 12 months and 18% after 24 months; after 24 months, 54% had ΔE values above 6.8 [2]. The clinical study proposed early glaze detachment as one possible explanation for discoloration of the exposed restoration surface, but the glaze layer itself was not examined [2]. In the present in vitro study, visible stain was retained mainly within the glaze, and glaze detachment, which was absent in the water-stored controls, was observed after immersion in curry and red wine even in the absence of mechanical loading. Because clinical color measurements were obtained on buccal and labial surfaces, which are less directly affected by occlusal wear [2], chemical or medium-related changes in the glaze could contribute to discoloration alongside mechanical influences. On occlusal surfaces, wear may further compromise the glazed surface. In the same clinical setting, mean profile loss reached 0.22 mm after 24 months; even non-fractured restorations showed mean losses of 0.07–0.09 mm after 12 and 24 months [25], values greater than the stained glaze layer thickness measured here (14.4–63.8 µm). The combined clinical and in vitro observations are therefore consistent with the possibility that the protective effect of the glaze is time-limited, and that deterioration of the glazed surface contributes to the discoloration observed clinically. This interpretation is compatible with the recommendation to limit the duration of use of these restorations [2,25] and with the suggestion that future studies evaluate mechanical polishing as an alternative surface treatment [25]. Future studies should therefore compare alternative surface finishing approaches, such as multistep mechanical high-gloss polishing, glazes or coatings of different chemistry or filler content, application of the glaze before final post-curing [23], and periodic renewal of the glaze, with regard to both color stability and coating durability.

4.6. Limitations

Several limitations should be considered. Only one specimen per group was sectioned, so the cross-sectional analysis is descriptive and differences among materials or staining media were not tested inferentially. The observed differences may therefore reflect specimen-specific variation and should not be generalized; future studies should include several sectioned specimens per group to confirm these patterns. Cross-sectional findings were compared with group means of ΔE_{00} and Ra rather than with measurements from the same individual specimen. Only one water-stored glazed control per material was sectioned, and in two materials (VE, CS) the glaze–substrate boundary could not be reliably delineated. Because the controls had been stored in water for 30 days, they do not

represent the glaze immediately after application. Pre-existing defects and immersion-induced alterations can therefore be distinguished only approximately, and future studies should include sections obtained before immersion. Continuous immersion for 30 days represents a more severe exposure than intermittent intake in vivo, where saliva, oral hygiene and dilution reduce contact time; the findings should therefore be regarded as a worst-case scenario rather than a direct prediction of clinical performance. Moreover, the extrapolation from immersion time to clinical exposure is only approximate, because the actual relationship depends on the chemistry and concentration of the staining agent, the frequency and duration of intake, saliva composition and flow, temperature changes and oral hygiene; the equivalence of 30 days to approximately 2.5 years should therefore be regarded as a rough orientation only. Similarly, coffee was prepared at a typical beverage concentration (10 g/L), and cola and red wine were used as consumed, whereas the curry suspension (approximately 5 g/L) was prepared empirically and does not represent a standardized dietary exposure. Combined or sequential exposure to different staining agents, as occurs with everyday dietary habits, was not investigated and should be considered in future studies. Mechanical loading, thermocycling and toothbrushing were not simulated. The immersion protocol was intended to isolate the chemical effect of the staining media on the glaze; however, thermal stresses and abrasion are likely to promote cracking, wear and detachment of the glaze in vivo, as indicated by the clinically observed profile loss [25]. The present findings may therefore underestimate the extent of glaze deterioration under clinical conditions, and future studies should use a more realistic intermittent protocol, for example, by alternating short daily exposures to the staining media with storage in artificial saliva or another reference medium, combined with thermocycling, toothbrushing and chewing simulation. The specimens were immersed without prior water conditioning, and distilled water rather than artificial saliva was used as storage and control medium. Water sorption therefore occurred concurrently with exposure to the staining media, which may have facilitated the uptake of chromogens into the glaze; moreover, salivary proteins and pellicle formation may modify staining and glaze degradation in vivo. Only two additively manufactured materials were included, limiting generalization to other 3D-printed restorative systems. The microscopic evaluation primarily detects visible discoloration; small amounts of chromogens within the substrate cannot be excluded, and chemical, spectroscopic or fluorescence-based methods would be required to determine actual chromogen penetration. The specimens were cleaned after grinding but not again after polishing or glazing, so residues from surface finishing cannot be completely excluded. However, the water-stored controls underwent identical preparation and showed irregular glaze contours but no detachment, which suggests that preparation-related features can be distinguished at least approximately from alterations associated with exposure to the staining media. SEM combined with energy-dispersive X-ray spectroscopy was not used for this purpose, because the chromogens of the staining media are predominantly organic compounds composed of the same elements as the resin-based glaze and matrix and would therefore not be expected to be reliably distinguished by elemental analysis; Raman or infrared mapping would be more suitable. Nevertheless, cross-sectional SEM would provide complementary high-resolution information on the morphology of the glaze and the glaze–substrate interface, such as microcracks, porosity, interfacial gaps and early debonding, which may not be resolved by light microscopy; combining light-optical and electron microscopy in future studies would therefore allow a more thorough characterization of immersion-related microstructural alterations. In addition, the color profiles were derived from uncalibrated microscope images, so differences in illumination and light scattering from the stained glaze into the translucent substrate may have influenced the measured gradients. Differences in translucency, filler content, and microstructure among the materials may additionally have affected light

propagation within the substrate. The color profiles should therefore be regarded as hypothesis-generating; calibrated imaging with a color reference standard combined with chemical or fluorescence-based analyses would be required to confirm substrate staining. The glaze alteration score was semi-quantitative, and inter-examiner agreement was only fair (linear weighted $\kappa = 0.25$), mainly reflecting difficulty in distinguishing adjacent categories; in addition, the second examiner evaluated one image per specimen. The scores should therefore be interpreted as an approximate descriptive classification. Finally, OPTIGLAZE was used for all materials although it is primarily indicated for resin-based substrates; the findings therefore apply specifically to the glazing protocol investigated here.

5. Conclusions

Within the limitations of this descriptive in vitro study, in which one specimen per group was sectioned, visible staining of glazed milled and 3D-printed hybrid materials after 30 days of immersion was located predominantly within the glaze layer. After curry exposure, exploratory color profiles suggested additional near-surface yellowing in some materials, particularly beneath detached glaze, whereas polished specimens showed no distinct visually discolored subsurface zone. Structural defects of the glaze were common, and detachment was observed in single specimens after curry and red wine exposure; material- or medium-specific differences could not be tested statistically and require confirmation in larger samples. Neither stained-layer thickness nor detachment corresponded consistently with the previously reported color change or surface roughness. Cross-sectional microscopy therefore adds information on glaze condition that surface color and roughness measurements alone do not provide. When considered together with clinical observations for the same 3D-printed material, the present data are consistent with the possibility that the protective effect of the glaze is time limited. Future studies should include multiple sections per group, glaze thickness measurements before immersion, and chemical or fluorescence-based methods to evaluate chromogen penetration.

Supplementary Materials: The following supporting information can be downloaded at: https://www.mdpi.com/article/10.3390/jfb17120595/s1, Figure S1: Cross-sections of the water-stored glazed control specimens; Figure S2: Representative cross-sections of VE; Figure S3: Representative cross-sections of CS; Figure S4: Representative cross-sections of VG; Figure S5: Representative cross-sections of 3D1; Figure S6: Representative cross-sections of 3D2; Figure S7: Color profiles after cola immersion; Figure S8: Color profiles after coffee immersion; Figure S9: Color profiles after red wine immersion; Figure S10: Scanning electron micrographs of the glazed and polished specimen surfaces; Table S1: Near-surface color differences of the substrate for all staining media; Supplementary Data: data files, R scripts (data preparation and Table 2) and Python script (color profiles).

Author Contributions: Conceptualization, J.Y.; methodology, J.Y.; investigation, J.Y., S.D., and E.P.; formal analysis, J.Y.; writing—original draft preparation, J.Y.; writing—review and editing, J.Y., F.B., E.P.; supervision, F.B. and E.P. All authors have read and agreed to the published version of the manuscript.

Funding: This research received no external funding. The materials were provided by the manufacturers, who had no role in study design, data collection, analysis, interpretation or manuscript preparation.

Institutional Review Board Statement: Not applicable.

Informed Consent Statement: Not applicable.

Data Availability Statement: The data, R scripts and Python script supporting the findings of this study are available in the Supplementary Materials and from the corresponding author upon reasonable request.

Acknowledgments: During the preparation of this manuscript, ChatGPT (**GPT-6,** OpenAI) and Claude (**Opus 5.5,** Anthropic) were used to assist with language editing.

Conflicts of Interest: The authors declare no conflicts of interest.

References

1. Arif, R.; Yilmaz, B.; Johnston, W.M. In vitro color stainability and relative translucency of CAD-CAM restorative materials used for laminate veneers and complete crowns. *J. Prosthet. Dent.* **2019**, *122*, 160–166.
2. Doumit, M.; Beuer, F.; Böse, M.W.H.; Nicic, R.; Hey, J.; Prause, E. The colour stability of 3D-printed, non-invasive restorations after 24 months in vivo—Esthetically pleasing or not? *J. Dent.* **2024**, *150*, 105391. https://doi.org/10.1016/j.jdent.2024.105391.
3. Kim, J.E.; Choi, W.H.; Lee, D.; Shin, Y.; Park, S.H.; Roh, B.D.; Kim, D. Color and translucency stability of three-dimensional printable dental materials for crown and bridge restorations. *Materials* **2021**, *14*, 650. https://doi.org/10.3390/ma14030650.
4. Spitznagel, F.A.; Vuck, A.; Gierthmühlen, P.C.; Blatz, M.B.; Horvath, S.D. Adhesive bonding to hybrid materials: An overview of materials and recommendations. *Compend. Contin. Educ. Dent.* **2016**, *37*, 630–637.
5. Kessler, A.; Hickel, R.; Reymus, M. 3D Printing in Dentistry—State of the Art. *Oper. Dent.* **2020**, *45*, 30–40. https://doi.org/10.2341/18-229-L.
6. Acar, O.; Yilmaz, B.; Altintas, S.H.; Chandrasekaran, I.; Johnston, W.M. Color stainability of CAD/CAM and nanocomposite resin materials. *J. Prosthet. Dent.* **2016**, *115*, 71–75.
7. Diken Türksayar, A.A.; Baytur, S. Color stability, surface roughness and flexural strength of additively manufactured and milled interim restorative materials after aging. *Odontology* **2023**, *111*, 680–686.
8. Arocha, M.A.; Basilio, J.; Llopis, J.; Di Bella, E.; Roig, M.; Ardu, S.; Mayoral, J.R. Colour stainability of indirect CAD-CAM processed composites vs. conventionally laboratory processed composites after immersion in staining solutions. *J. Dent.* **2014**, *42*, 831–838. https://doi.org/10.1016/j.jdent.2014.04.002.
9. Gupta, G.; Gupta, T. Evaluation of the effect of various beverages and food material on the color stability of provisional materials—An in vitro study. *J. Conserv. Dent.* **2011**, *14*, 287–292.
10. Almejrad, L.; Yang, C.C.; Morton, D.; Lin, W.S. The effects of beverages and surface treatments on the color stability of 3D-printed interim restorations. *J. Prosthodont.* **2022**, *31*, 165–170.
11. Al-Shami, A.M.; Alshami, M.A.; Al-Kholani, A.I.; Al-Sayaghi, A.M. Color stability of nanohybrid and microhybrid composites after immersion in common coloring beverages at different times: A laboratory study. *BDJ Open* **2023**, *9*, 39. https://doi.org/10.1038/s41405-023-00161-9.
12. Çakmak, G.; Oosterveen-Rüegsegger, A.L.; Akay, C.; Schimmel, M.; Yilmaz, B.; Donmez, M.B. Influence of polishing technique and coffee thermal cycling on the surface roughness and color stability of additively and subtractively manufactured resins used for definitive restorations. *J. Prosthodont.* **2024**, *33*, 467–474.
13. Gönülol, N.; Yilmaz, F. The effects of finishing and polishing techniques on surface roughness and color stability of nanocomposites. *J. Dent.* **2012**, *40*, e64–e70. https://doi.org/10.1016/j.jdent.2012.07.005.
14. Sagsoz, O.; Demirci, T.; Demirci, G.; Sagsoz, N.P.; Yildiz, M. The effects of different polishing techniques on the staining resistance of CAD/CAM resin-ceramics. *J. Adv. Prosthodont.* **2016**, *8*, 417–422. https://doi.org/10.4047/jap.2016.8.6.417.
15. Sarıkaya, I.; Yerliyurt, K.; Hayran, Y. Effect of surface finishing on the colour stability and translucency of dental ceramics. *BMC Oral Health* **2018**, *18*, 40. https://doi.org/10.1186/s12903-018-0508-4.
16. Lask, M.; Mayinger, F.; Reymus, M.; Meinen, J.; Stawarczyk, B. Impact of glazing, coating, and polishing on the color stability and surface properties of a 3D printed resin and two veneering composite resins. *J. Esthet. Restor. Dent.* **2025**, *37*, 1814–1826.
17. Angwaravong, O.; Sirichay, S.; Pengsuk, T.; Sooksuwan, P.; Angwarawong, T. Effect of surface coating, thermocycling, and staining solutions on the color stability of CAD-CAM polymethyl methacrylate interim fixed restorations. *J. Esthet. Restor. Dent.* **2025**, *37*, 2270–2280.
18. Nam, N.-E.; Hwangbo, N.-K.; Kim, J.-E. Effects of surface glazing on the mechanical and biological properties of 3D printed permanent dental resin materials. *J. Prosthodont. Res.* **2024**, *68*, 273–282. https://doi.org/10.2186/jpr.JPR_D_22_00261.

19. Sabanik, P.; Liu, T.-C.; Tabatabaeian, M.; Rocha, M.G.; Surathu, N.; Lawson, N.C. A Review of Current Systems, Materials, and Protocols for 3D-Printed Splints, Crowns, and Dentures. *J. Esthet. Restor. Dent.* **2026**, *38*, 635–651. https://doi.org/10.1111/jerd.70125.
20. Espinar, C.; Della Bona, A.; Tejada-Casado, M.; Pulgar, R.; Pérez, M.M. Optical behavior of 3D-printed dental restorative resins: Influence of thickness and printing angle. *Dent. Mater.* **2023**, *39*, 894–902. https://doi.org/10.1016/j.dental.2023.08.003.
21. Souza, L.D.S.; Mendoza, A.; Caneppele, T.M.F.; Sellan, P.L.B.; Bresciani, E. Influence of printing orientation and post-curing on optical and surface properties of definitive three-dimensional-printed dental resin with inorganic fillers. *Eur. J. Oral Sci.* **2026**, *134*, e70083. https://doi.org/10.1111/eos.70083.
22. Kalyoncuoğlu, Ü.T.; Yilmaz Erdemli, B.; Ayyildiz, S. Diet-Induced Chromogenic Challenge Model for Additively Manufactured Tooth-Colored Dental Resin Materials. *J. Esthet. Restor. Dent.* **2026**.(Early View: 2026; 0:1–11) https://doi.org/10.1111/jerd.70257.
23. Narin, A.; Ezmek, B. Effect of modified glaze application protocols on color stability of 3D-printed permanent dental resins. *BMC Oral Health* **2026**, *26*, 1747. https://doi.org/10.1186/s12903-026-08972-6.
24. Yassine, J.; Beuer, F.; Debes, S.; Schmidt, F.; Yassine, B.; Prause, E. Does manufacturing technique matter? Color stability, surface roughness, and microstructural changes of 3D-printed versus milled hybrid dental materials: An in vitro study. *Clin. Exp. Dent. Res.* 2026, *under review*.
25. Doumit, M.; Beuer, F.; Böse, M.W.H.; Unkovskiy, A.; Hey, J.; Prause, E. Wear behavior of 3D printed, minimally invasive restorations: Clinical data after 24 months in function. *J. Prosthet. Dent.* **2025**, *134*, 662–669. https://doi.org/10.1016/j.prosdent.2025.03.014.
26. Ertaş, E.; Güler, A.U.; Yücel, A.Ç.; Köprülü, H.; Güler, E. Color stability of resin composites after immersion in different drinks. *Dent. Mater. J.* **2006**, *25*, 371–376. https://doi.org/10.4012/dmj.25.371.
27. Salah El Din, M.W.M.; Tawfik, A.K.; Wahsh, M.M. Effect of different storage media on the surface roughness of two CAD/CAM materials. *Ain Shams Dent. J.* **2021**, *21*, 1–11. https://doi.org/10.21608/asdj.2021.53197.1002.

Disclaimer/Publisher's Note: The statements, opinions and data contained in all publications are solely those of the individual author(s) and contributor(s) and not of MDPI and/or the editor(s). MDPI and/or the editor(s) disclaim responsibility for any injury to people or property resulting from any ideas, methods, instructions or products referred to in the content.